© 2014. Published by The Company of Biologists Ltd | Journal of Cell Science (2014) 127, 5149–5156 doi:10.1242/jcs.152579

SHORT REPORT

TRAIP is a regulator of the spindle assembly checkpoint

Christophe Chapard[1], Patrick Meraldi[2], Tobias Gleich[1], Daniel Bachmann[1], Daniel Hohl[1] and Marcel Huber[1,*]

ABSTRACT

Accurate chromosome segregation during mitosis is temporally and spatially coordinated by fidelity-monitoring checkpoint systems. Deficiencies in these checkpoint systems can lead to chromosome segregation errors and aneuploidy, and promote tumorigenesis. Here, we report that the TRAF-interacting protein (TRAIP), a ubiquitously expressed nucleolar E3 ubiquitin ligase important for cellular proliferation, is localized close to mitotic chromosomes. Its knockdown in HeLa cells by RNA interference (RNAi) decreased the time of early mitosis progression from nuclear envelope breakdown (NEB) to anaphase onset and increased the percentages of chromosome alignment defects in metaphase and lagging chromosomes in anaphase compared with those of control cells. The decrease in progression time was corrected by the expression of wild-type but not a ubiquitin-ligase-deficient form of TRAIP. TRAIP-depleted cells bypassed taxol-induced mitotic arrest and displayed significantly reduced kinetochore levels of MAD2 (also known as MAD2L1) but not of other spindle checkpoint proteins in the presence of nocodazole. These results imply that TRAIP regulates the spindle assembly checkpoint, MAD2 abundance at kinetochores and the accurate cellular distribution of chromosomes. The TRAIP ubiquitin ligase activity is functionally required for the spindle assembly checkpoint control.

KEY WORDS: TRAF-interacting protein, TRAIP, Mitosis, Chromosome mis-segregation, Spindle assembly checkpoint

INTRODUCTION

The equal distribution of chromosomal DNA during mitosis is ensured by a highly complex process in which the control of APC/C (anaphase-promoting complex/cyclosome) activity is crucial (Foley and Kapoor, 2013; Kops et al., 2005; Pines, 2011). APC/C activity is regulated by the spindle assembly checkpoint (SAC) proteins MAD1, MAD2 (also known as MAD1L1, MAD2L1, respectively), BUBR1 (also known as BUB1B), BUB1, BUB3 and MPS1 (also known as TTK), which sense whether or not chromosomes are connected in a bi-oriented manner to opposite spindle poles through microtubules (Foley and Kapoor, 2013; Khodjakov and Pines, 2010; Santaguida and Musacchio, 2009). The strength of the SAC crucially depends on the MAD2 abundance at kinetochores (Collin et al., 2013; Heinrich et al., 2013). Defects in chromosome segregation control cause chromosomal instability and aneuploidy, common characteristics of human solid tumors (Holland and Cleveland, 2012).

Ubiquitylation is a highly conserved biochemical process during which ubiquitin monomers are attached to proteins (Dikic et al., 2009; Welchman et al., 2005). The TNF-receptor-associated factor (TRAF)-interacting protein (TRAIP, also known as TRIP or RNF206) is a RING-type E3 ubiquitin ligase (Besse et al., 2007), but hitherto no *in vivo* substrate has been identified. Ectopically expressed TRAIP interacts with TRAF proteins and represses NF-κB signaling (Besse et al., 2007; Lee et al., 1997), although this might not be physiologically relevant (Chapard et al., 2012). TRAIP is expressed ubiquitously at a low level (Lee et al., 1997; Su et al., 2004) in the nucleoli (Zhou and Geahlen, 2009) of interphase cells but is overexpressed in breast cancer cell lines (Zhou and Geahlen, 2009) and in basal cell carcinomas (Almeida et al., 2011).

Both TRAIP-knockout mice (Park et al., 2007) and mutants of NOPO (Merkle et al., 2009), the *Drosophila* homolog of mammalian TRAIP, die early in development owing to aberrant proliferation and mitosis. TRAIP transcription is strongly downregulated upon induction of cell cycle exit, and its knockdown decreases proliferation and causes a G1/S phase block in keratinocytes (Almeida et al., 2011). TRAIP interacts with CYLD (Regamey et al., 2003) and SYK (Zhou and Geahlen, 2009), two tumor suppressors (Bailet et al., 2009; Bignell et al., 2000; Coopman et al., 2000; Lee et al., 2005; Moroni et al., 2004), and with DNA polymerase η, which facilitates translesional synthesis after DNA damage (Wallace et al., 2014).

We report here that the TRAIP protein preferentially localizes during mitosis around condensed chromosomes in prometaphase and metaphase, and on chromosomal DNA in anaphase. Its functional inactivation accelerates the progression through early phases of mitosis, reduces MAD2 recruitment to kinetochores and leads to increased mitotic defects. Our findings strongly support the existence of a role for TRAIP in SAC regulation.

RESULTS AND DISCUSSION

TRAIP preferentially localizes at the periphery of chromosomes in early mitosis

Analysis of endogenous TRAIP expression by immunofluorescence detection in mitotic cells showed localization around prometaphase chromosomes and colocalization with anaphase chromosomes (Fig. 1A). To determine the specificity of the antibody, immune detection of endogenous TRAIP in HeLa cells was analyzed 24 h after transfection with two small interfering (si)RNAs targeting TRAIP (siTRAIP1 and siTRAIP2) or a scrambled negative control siRNA (siCTRL). TRAIP mRNA and protein levels were reduced to ∼30% in TRAIP-depleted cells compared with levels in control cells (supplementary material Fig. S1A). The immunofluorescent signal of endogenous TRAIP was observed in the nucleoplasm of both siCTRL- and siTRAIP-treated cells during interphase (Fig. 1B). After treatment of cells with a short detergent extraction before fixation, to remove soluble proteins (Nalepa

[1]Service of Dermatology, Lausanne University Hospital, CHUV, 1011 Lausanne, Switzerland. [2]Department of Cell Physiology and Metabolism, University of Geneva, 1211 Geneva, Switzerland.

*Author for correspondence (marcel.huber@chuv.ch)

Received 4 March 2014; Accepted 10 October 2014

Journal of Cell Science

Journal of Cell Science (2014) 127, 5149–5156 doi:10.1242/jcs.152579

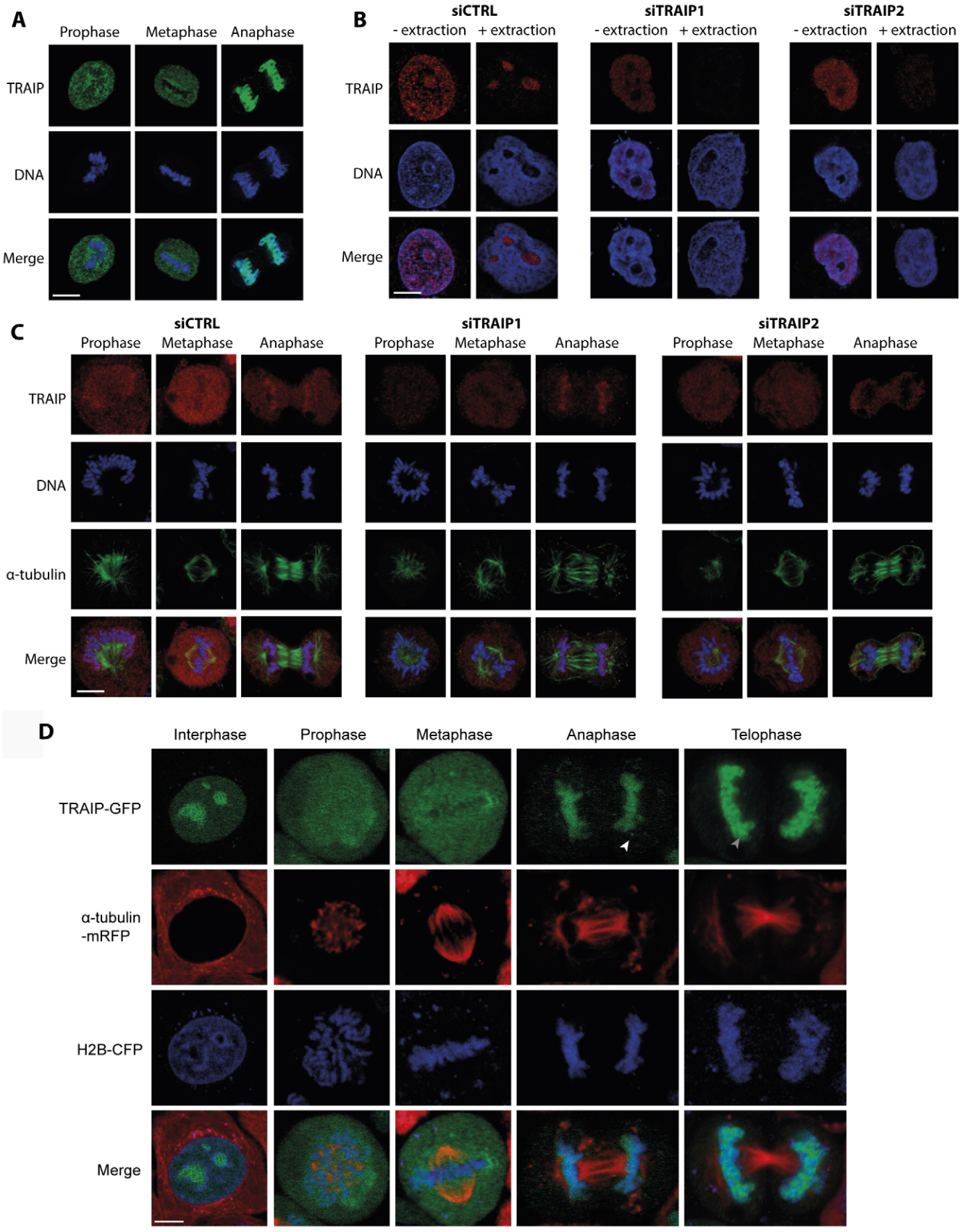

Fig. 1. See next page for legend.

Journal of Cell Science

Journal of Cell Science (2014) 127, 5149–5156 doi:10.1242/jcs.152579

Fig. 1. Endogenous and ectopic TRAIP is a chromosomal peripheral protein during mitosis. (A) Confocal images of mitotic HeLa cells immunostained with anti-TRAIP antibody (green). (B,C) Confocal images of HeLa cells in interphase (B) or mitosis (C) immunostained for endogenous TRAIP (red) and α-tubulin (green), 24 h after treatment with the indicated siRNAs. Extraction was carried out with 0.1% Triton X-100 for 2 min before fixation (B). The settings for confocal imaging were identical within experiments. DNA was stained with DAPI (blue). (D) Confocal images of living HeLa cells stably expressing α-tubulin–mRFP (red) and H2B–CFP (blue) together with TRAIP–GFP (green). PNB and NDF are marked by gray and white arrowheads, respectively. Scale bars: 5 μm.

et al., 2013), the signal became nucleolar in controls and disappeared from TRAIP-depleted cells. The signal in mitotic cells was localized close to congressing chromosomes in prometaphase and was associated with condensed chromosomes in anaphase in controls but was strongly reduced in siTRAIP-treated cells (Fig. 1C).

To further validate TRAIP localization, a lentiviral vector driving expression of a functional (supplementary material Fig. S2; Besse et al., 2007; Zhou and Geahlen, 2009) TRAIP–GFP was used to infect HeLa cells stably expressing α-tubulin–mRFP and H2B–CFP (Beronja et al., 2010). In early mitotic phases, TRAIP–GFP was dispersed throughout the cytoplasm and converged at the chromosome periphery, whereas in later phases it colocalized with chromosomes (Fig. 1D). During telophase, a small fraction accumulated in cytoplasmic particles, probably corresponding to nucleolus-derived foci (NDF) and pre-nucleolar bodies (PNB) (Dundr et al., 1997; Ma et al., 2007; Van Hooser et al., 2005).

The perichromosomal layer of TRAIP appeared in prometaphase and disappeared in telophase or cytokinesis (Hernandez-Verdun and Gautier, 1994; Ma et al., 2007; Van Hooser et al., 2005). Nucleolar proteins and RNAs are known to bind to the surface of chromosomes at the beginning of mitosis and are incorporated again into newly formed nucleoli during telophase (Dundr et al., 1997; Van Hooser et al., 2005). Different biological functions have been assigned to chromosomal peripheral proteins (CPP) forming the perichromosomal layer (Hernandez-Verdun, 2011; Hernandez-Verdun and Gautier, 1994; Ma et al., 2007; Matsunaga and Fukui, 2010). Our analysis identified the nucleolar protein TRAIP as a CPP and prompted us to investigate TRAIP function in mitosis.

TRAIP regulates progression through early phases of mitosis

We examined the consequences of silencing TRAIP expression on the duration of mitosis using siRNAs and fluorescence time-lapse imaging of HeLa cells expressing H2B–EGFP and α-tubulin–mRFP (Toso et al., 2009), taking nuclear envelope breakdown (NEB) as starting time, $t=0$ min (Meraldi et al., 2004). In siCTRL-transfected cells, the median duration of mitosis was 116.7 min [95% confidence interval (CI)=111.7–123.3 min; range, 75 to 275 min]. The high variability of duration of mitosis was mainly caused by the time between NEB to anaphase onset (Lim et al., 2013; Mchedlishvili et al., 2012; Rieder et al., 1994; Toso et al., 2009), which varied from 20 to 200 min (median, 53.3 min; 95% CI=46.7–61.7 min). The time from anaphase to cytokinesis fluctuated only moderately from 45 to 85 min (median, 63.3 min; 95% CI=60–66.7 min) (Fig. 2A–D).

The average time taken to complete mitosis by siTRAIP1- or siTRAIP2-treated cells was reduced to 96.7 min (95% CI=95–101 min) or 90 min (95% CI=87.7–91.7 min), respectively (Fig. 2A). Although the time from anaphase to cytokinesis with siTRAIP1 (range, 45 to 95 min; median, 66.7 min; 95% CI=63.3–70 min) and siTRAIP2 (range, 45 to 80 min; median, 58.3 min; 95% CI=56.7–63.3 min) was very similar to that of control cells, the time from NEB to anaphase onset was significantly reduced to 30 min (95% CI=28.3–33.3 min; range, 20 to 75 min) with siTRAIP1 and 26.7 min (95% CI=26.7–28.3 min; range, 20 to 85 min) with siTRAIP2 (Fig. 2B,C). In total, 90% of TRAIP-depleted cells accomplished the onset of anaphase within 45 min after NEB compared to only 50% of control cells (Fig. 2E). In the skew-normal frequency distribution of anaphase onset times, a first population (peak of the distribution) with rapid and uniform chromosome congression and a second with longer anaphase onset times (active spindle checkpoint) could be distinguished (Meraldi et al., 2004; Rieder et al., 1994). In control siRNA-transfected HeLa cells, the skew-normal distribution of anaphase onset times had a peak (mode) at 31.8±1.2 min, whereas in TRAIP-depleted cells a shift to 28.4±0.4 min (siTRAIP1; mean±s.e.m.) or 24.2±0.4 min (siTRAIP2) was observed (Fig. 2F). The NEB to anaphase onset time in cells transduced with siRNA-resistant TRAIP before siRNA transfection was indistinguishable from that of the control, whereas a catalytically inactive TRAIP mutant (C25A) failed to rescue the siRNA-treated cells (Fig. 2G). Although MAD2 is a frequent siRNA off-target (Hübner et al., 2010; Sigoillot et al., 2012; Westhorpe et al., 2010), the expression of MAD2, MAD1, BUB1 and BUB3 remained unchanged after TRAIP KD (supplementary material Fig. S1B,C). Taken together with the rescue data it is therefore unlikely that TRAIP-knockdown phenotypes are caused by off-target effects. These findings suggest that the ubiquitin ligase TRAIP is involved in the regulation of NEB to anaphase onset time.

TRAIP loss increases the occurrence of chromosome alignment defects and lagging chromosomes

Because a reduced NEB to anaphase onset time could induce aberrant chromosome segregation (Meraldi and Sorger, 2005; Michel et al., 2001; Perera et al., 2007), we examined whether TRAIP depletion affected chromosome behavior. Following TRAIP depletion, the number of cells dividing with a bipolar spindle and giving rise to two living daughter cells was not significantly different from that of control cells. Mitotic indexes in siRNA-treated cells were examined by immunostaining with anti-phospho-histone H3(Ser28) and anti-α-tubulin antibodies. Although mitotic indexes were comparable to those of controls (Fig. 3A), the percentage of cells in prophase was reduced by 10–20% in TRAIP-depleted compared with control cells (Fig. 3B), consistent with shorter NEB to anaphase onset times. In TRAIP-depleted mitotic cells synchronized by a double-thymidine block, the percentage of non-aligned chromosomes at the metaphase plate was increased compared with that of the control (siRNA1, 38.5±4.9%; siRNA2, 37.1±7.6%; control, 19.6±7.5%; mean±s.d) (Fig. 3C,E). More chromosome segregation errors were detected in mitotic cells treated with either siTRAIP1 or 2 compared with the number observed in control cells (15.7±4.5% or 19.5±6.7% versus 9.7±2.9%; mean±s.d.) (Fig. 3D,F). As expected, the number of chromosome alignment and segregation errors was increased in MAD2-depleted cells, supporting the reliability of our data (Fig. 3E,F). In summary, TRAIP downregulation in HeLa cells leads to chromosome misalignment and segregation defects.

Journal of Cell Science (2014) 127, 5149–5156 doi:10.1242/jcs.152579

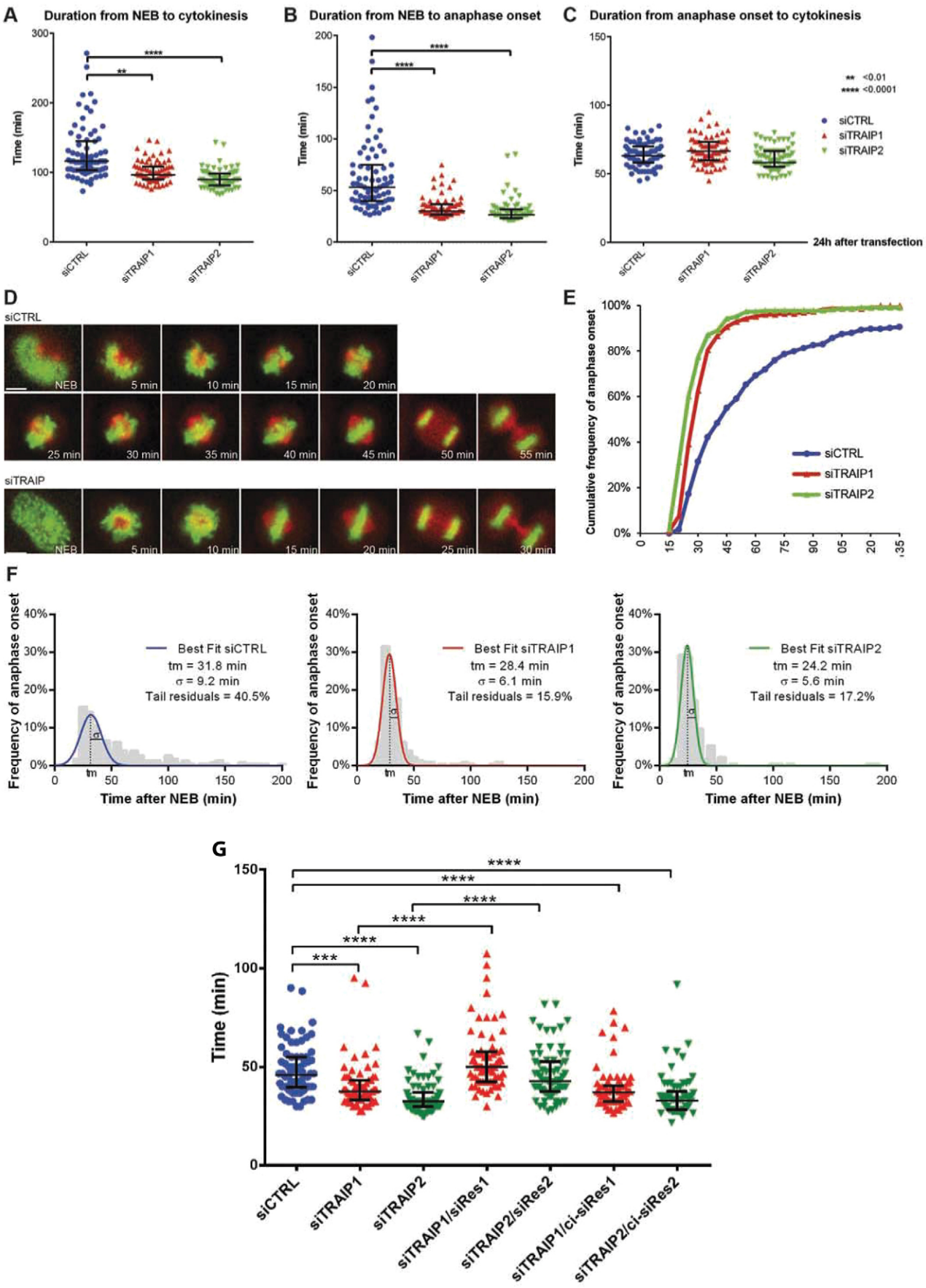

Fig. 2. See next page for legend.

Journal of Cell Science (2014) 127, 5149–5156 doi:10.1242/jcs.152579

Fig. 2. TRAIP depletion decreases the NEB to anaphase time. (A–C) Scatter plots (indicating the median and interquartile range) of times taken to complete mitosis (A), times from NEB to anaphase onset (B) and from anaphase onset to cytokinesis (C) in siRNA-treated HeLa cells. $N=3$ independent experiments, $n=225$ cells. (D) Successive frames from live-cell movies. Red, α-tubulin; green, histone 2B. Scale bar: 5 μm. (E) Cumulative frequency plots of anaphase onset times (NEB=0 min). $N=3$ independent experiments, $n=225$ cells. (F) Frequency distribution of anaphase onset times. $N=3$ independent experiments, $n=225$ cells. (G) The decrease in NEB to anaphase onset time was rescued by the expression of siRNA-resistant wild-type but not by catalytically inactive (ci, C25A) TRAIP. The median and interquartile range are indicated; $N=3$ independent experiments, $n=180$ cells. $^{**}P<0.01$, $^{***}P<0.001$, $^{****}P<0.0001$.

TRAIP loss decreases SAC function

Our results demonstrated that early mitosis and chromosome behavior are affected by TRAIP knockdown, suggesting a role of TRAIP in the SAC. To investigate whether TRAIP knockdown enabled HeLa cells to bypass the SAC, a taxol-induced mitotic arrest assay (Stegmeier et al., 2007a) was undertaken to assess mitotic index and nuclear morphology. CYLD- and MAD2-specific siRNAs were used as controls for mitotic entry delay and SAC bypass (Draviam et al., 2007; Meraldi et al., 2004; Stegmeier et al., 2007a; Stegmeier et al., 2007b). Only 13±8% (mean±s.d.) of MAD2-depleted or 51±15% of CYLD-depleted cells were mitotic (Fig. 4A,B) (Stegmeier et al., 2007b), whereas the value was higher for control cells (74±7%). In TRAIP-depleted cells, a reduced mitotic index (siRNA1, 52±16%; siRNA2, 53±8%) (Fig. 4B) and multilobed nuclear morphology (Stegmeier et al., 2007a; Stegmeier et al., 2007b), similar to that of cells treated with MAD2-specific siRNA (Fig. 4A,C), was observed, demonstrating that loss of TRAIP led to a checkpoint-bypass phenotype. However, TRAIP depletion led to a smaller effect than MAD2 knockdown. Whether this reflects a phenotypic difference or is due to differences in the degree of mRNA knockdown remains to be seen. Our data indicated that TRAIP depletion was less effective compared with MAD2 knockdown (supplementary material Fig. S1A). To summarize, loss of TRAIP reduced mitotic arrest in response to the spindle poison taxol, hence leading to the bypass of the SAC.

TRAIP depletion decreases MAD2 levels at unattached kinetochores

The expression and/or localization of SAC proteins are finely modulated to regulate APC/C activity (Musacchio and Salmon, 2007) in a dose-dependent manner (Collin et al., 2013; Heinrich et al., 2013). The robustness of the SAC is, in part, determined by the amount of MAD2 recruited to kinetochores. To elucidate whether TRAIP deficiency is affecting the kinetochore localization

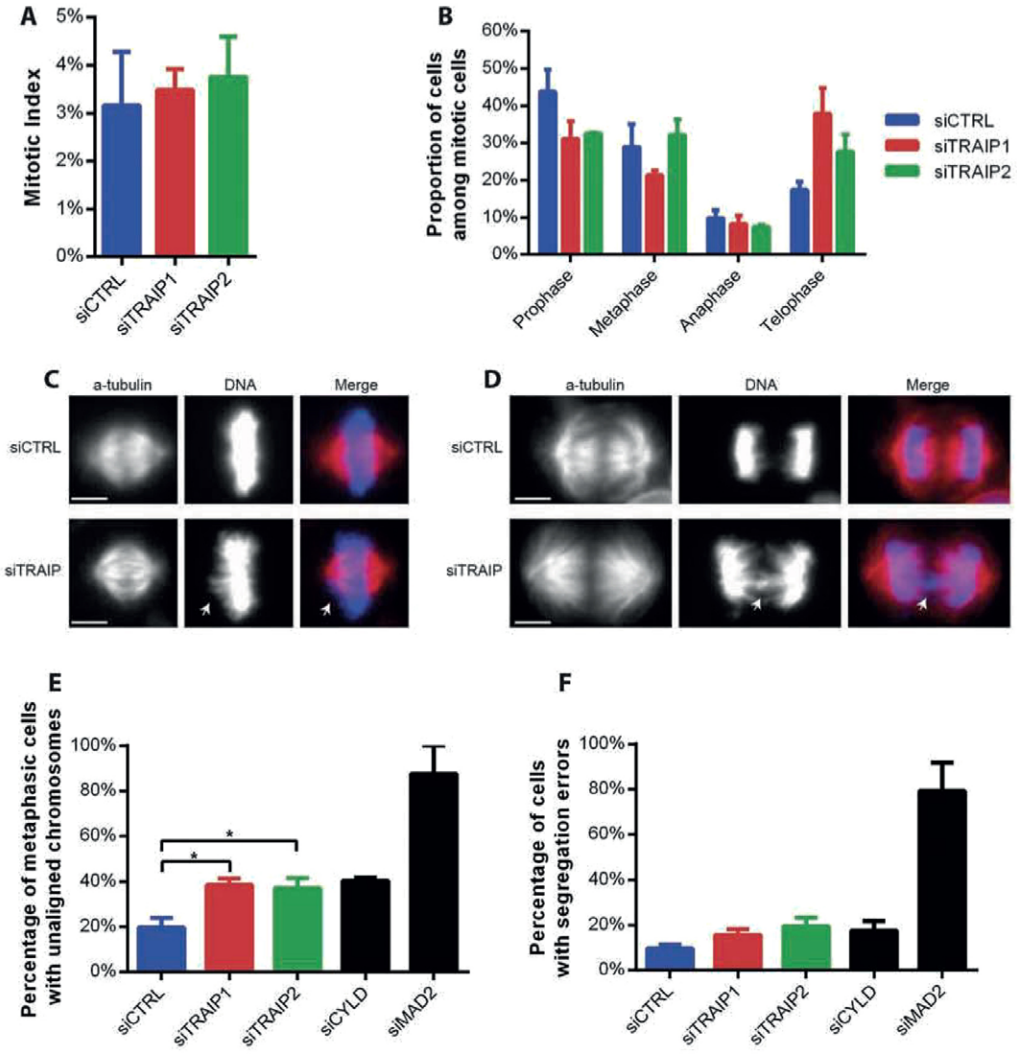

Fig. 3. TRAIP depletion leads to chromosome alignment defects and lagging chromosomes. (A) Mitotic index of siRNA-treated HeLa cells. $N=3$ independent experiments, $n=7000$ cells. (B) Distribution of siRNA-treated HeLa cells in the different phases of mitosis. $N=3$ independent experiments, $n=250$ cells. (C,D) Representative images of siRNA-transfected HeLa cells in metaphase (C) and anaphase (D). Arrows show unaligned (C) or lagging chromosomes (D). Scale bars: 5 μm. (E) Fraction of cells with unaligned chromosomes at the metaphase plate. $N=3$ independent experiments, $n>100$ (siCTRL, siTRAIP1 and siTRAIP2); $N=2$ independent experiments, $n=14$ cells (siMAD2) and 60 cells (siCYLD). (F) The fraction of cells with segregation errors in anaphase. $N=3$ independent experiments, $n>150$ cells (siCTRL, siTRAIP1 and siTRAIP2); $N=2$ independent experiments, $n=69$ cells (siMAD2) and 45 cells (siCYLD). Results in A,B,E,F are shown as the mean±s.e.m.

Journal of Cell Science (2014) 127, 5149–5156 doi:10.1242/jcs.152579

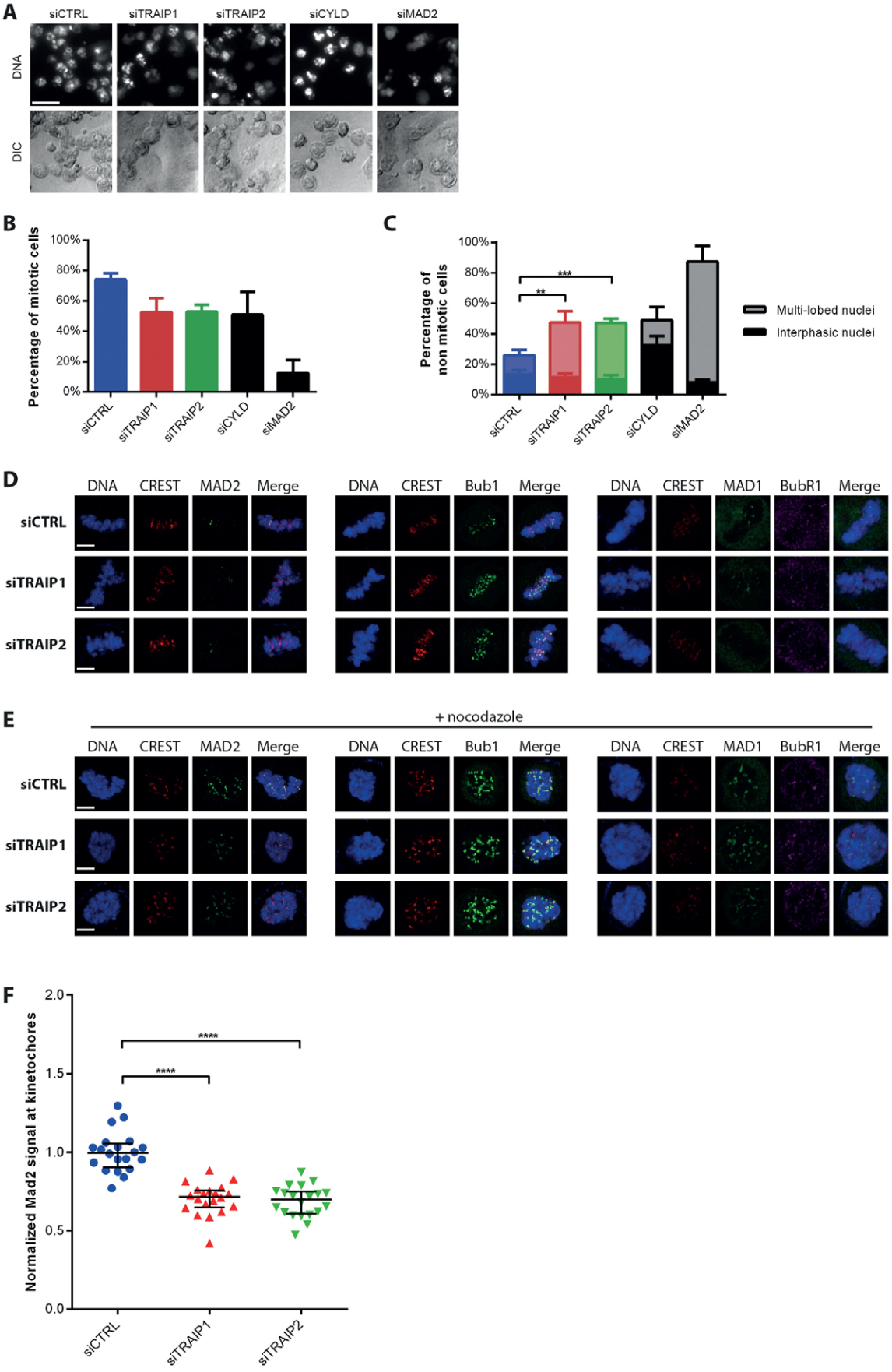

Fig. 4. See next page for legend.

Journal of Cell Science

Fig. 4. TRAIP knockdown affects the spindle checkpoint by reducing the amount of MAD2 at unattached kinetochores. (A) Representative images of siRNA-transfected HeLa cells treated with 100 nM taxol for 24 h. Scale bar: 30 μm. (B,C) The percentage of mitotic cells (B) and cells with either multilobed or interphase nuclei (C) was determined by cell rounding in DIC microscopy and DAPI staining. The results are represented as the mean±s.e.m. $N=4$ independent experiments, $n>2700$ cells (siCTRL, siTRAIP1 and siTRAIP2); $N=2$ independent experiments, $n=400$ cells (siMAD2 and siCYLD). (D,E) Confocal images of siRNA-treated HeLa cells immunostained for CREST (red) and either MAD1, MAD2, BUB1 (green) or BUBR1 (purple). Cells in E were treated with nocodazole (1 μg/ml) for 1 h prior to analysis. Scale bars: 5 μm. (F) Scatter plot of MAD2 intensities at single kinetochores in nocodazole-treated cells shown in E. Quantification of MAD2 levels relative to the CREST signal is shown, along with the median and interquartile range. The total mean signal for MAD2 in control cells was normalized to 1. $^{**}P<0.01$, $^{***}P<0.001$, $^{****}P<0.0001$.

of SAC proteins, we performed immunofluorescence detection of MAD1, MAD2, BUB1 and BUBR1 proteins in TRAIP-siRNA-treated cells (Fig. 4D,E). SAC proteins were correctly positioned at unattached kinetochores marked by an anti-CREST antibody in prometaphase cells. However, the amount of MAD2 recruited to the kinetochores was significantly reduced in TRAIP-depleted cells compared with that of control cells (siRNA1, 70.2%±10.1%; siRNA2, 68.5%±9.9%; control, 100%±12.8%; mean±s.d.) (Fig. 4E,F). This might be physiologically relevant, because a reduction of 20% in MAD2 levels is sufficient to impair SAC activity in yeast (Heinrich et al., 2013).

In summary, we have demonstrated that TRAIP changes its predominantly nucleolar localization in interphase cells to the perichromosomal layer in mitosis. The decrease in progression time from NEB to anaphase onset and in the binding of MAD2 to kinetochores in TRAIP-depleted cells, leading to chromosome misalignment and segregation errors, implicates TRAIP as a novel regulator of SAC activity that functions in a ubiquitin-ligase-dependent manner. Our findings most likely explain the cell death in TRAIP-knockout mice and NOPO mutants in *Drosophila* embryos, because inaccurate chromosome segregation negatively impinges on the life of normal cells. The elucidation of the mechanism by which TRAIP functions at the molecular level to regulate the SAC awaits identification of its substrates and interaction partners.

MATERIALS AND METHODS

Cell culture

Cells were cultured in DMEM containing 10% fetal bovine serum and appropriate antibiotics (200 μg/ml G418, 0.25 μg/ml puromycin). Cells were synchronized by a double-thymidine (2 mM) block. Transfection of siRNAs was performed after the first thymidine treatment.

Plasmids and lentivirus

TRAIP cDNA was amplified from a human cDNA library and cloned into pEGFP-N3 (Clontech) or the lentiviral vector pCDH-CMV-MCS-EF1-Hygro (BioCat). TRAIP cDNAs with the C25A mutation or resistance to siRNAs were constructed by PCR amplification. PCR products were verified by sequencing. LV-CFP expressing H2B–CFP was purchased (Addgene #25998). Lentivirus was produced as described previously (Wiznerowicz and Trono, 2003). Cells were infected (multiplicity of infection of 10) with lentivirus (Almeida et al., 2011) and selected with 800 μg/ml hygromycin.

Protein extractions and TRAIP autoubiquitylation

Proteins were extracted by cell lysis in 1% SDS in phosphate-buffered saline. For immunoblots, the following antibodies were used: anti-GFP (Clontech), anti-actin (Sigma), rabbit anti-TRAIP (Abcam), goat anti-TRAIP (Imgenex), anti-MAD2 (Covance) and anti-HA (Santa Cruz Biotechnology). TRAIP autoubiquitylation was carried out as described previously (Almeida et al., 2008). Signals from immunoblots were captured by using LAS4000 (GE Healthcare) and analyzed by using ImageJ.

RNA interference

siRNA targeting human TRAIP mRNA (NM_005879.2), CYLD (Draviam et al., 2007; Sun et al., 2010) and MAD2 (Uzunova et al., 2012), and control siRNA (Origene), were transfected into cells at a final concentration of 30 nM using INTERFERin (Polyplus).

Live-cell imaging and immunofluorescence analysis

Experiments were performed at 37℃ under 5% CO_2 in cell-culture chambers (MatTek) in Phenol-Red-free medium. For time-lapse experiments, 24 h after siRNA transfection, images were recorded every 5 min for 16 h using a 20× Plan-Neofluar NA 0.5 objective on a Axio Observer Z1 microscope (Zeiss). Confocal live-cell imaging experiments were performed using a 63×/1.4 oil objective on a LSM700 confocal laser-scanning microscope (Zeiss). Antibodies against the following proteins were used for immunofluorescence: GFP (Clontech), TRAIP (Abcam), phospho-histone H3(Ser28) (Cell Signaling Technology), tubulin (Sigma), nucleolin C23 (Santa Cruz Biotechnology), MAD1 (Meraldi et al., 2004), MAD2 (Bethyl Laboratories), BUB1 (Klebig et al., 2009), BUBR1 (Klebig et al., 2009) and CREST (Klebig et al., 2009). Images were analyzed using ImageJ. Kinetochore levels of MAD2 were quantified as described previously (McClelland et al., 2007).

Taxol assay

The taxol assay in HeLa cells was carried out as described previously (Stegmeier et al., 2007a), except for DNA staining with DAPI. MosaiX images were acquired using a 20× objective on an Axio Imager microscope (Zeiss) equipped with differential interference contrast (DIC) and DAPI filters. Cells were scored using ImageJ.

RNA isolation and qRT-PCR analysis

RNA was purified using the RNeasy Kit (Qiagen) and cDNA was synthesized using Primescript-RT Kit (TakaRa). Quantitative PCR analysis was performed (Almeida et al., 2011) using primers for RPL13A (endogenous reference), TRAIP, CYLD, MAD1, BUB1B, BUB3 (Qiagen) or MAD2 (Universal Probe Library, Roche).

Statistical analyses

Statistical significance ($^{*}P<0.05$, $^{**}P<0.01$, $^{***}P<0.001$, $^{****}P<0.0001$) was calculated using one-way ANOVA followed by Tukey's multiple comparisons test or two-way ANOVA followed by Tukey–Kramer's post hoc test (GraphPad Prism6).

Acknowledgements

We thank Elaine Fuchs (Howard Hughes Medical Institute, The Rockefeller University, New York, NY) for the LV-CFP plasmid, Didier Trono (Laboratory of Virology and Genetics, EPFL, Lausanne, Switzerland) for psPAX2 and pMD2.G plasmids and Florence Morgenthaler from the Cellular Imaging Facility, Lausanne University.

Competing interests

The authors declare no competing interests.

Author contributions

M.H. designed and supervised the present study. C.C., T.G. and D.B. performed experiments. C.C., P.M., D.H. and M.H. wrote and discussed the paper.

Funding

M.H. is supported by the Swiss National Science Foundation [grant number 31003A-138416]; and the Emma Muschamp Foundation. P.M. acknowledges support from the Swiss National Science Foundation [grant number 31003A-141256]; the University of Geneva; and the Louis-Jeantet Foundation.

Supplementary material

Supplementary material available online at
http://jcs.biologists.org/lookup/suppl/doi:10.1242/jcs.152579/-/DC1

References

Almeida, S., Maillard, C., Itin, P., Hohl, D. and Huber, M. (2008). Five new CYLD mutations in skin appendage tumors and evidence that aspartic acid 681 in CYLD is essential for deubiquitinase activity. *J. Invest. Dermatol.* **128**, 587-593.

Almeida, S., Ryser, S., Obarzanek-Fojt, M., Hohl, D. and Huber, M. (2011). The TRAF-interacting protein (TRIP) is a regulator of keratinocyte proliferation. *J. Invest. Dermatol.* **131**, 349-357.

Bailet, O., Fenouille, N., Abbe, P., Robert, G., Rocchi, S., Gonthier, N., Denoyelle, C., Ticchioni, M., Ortonne, J. P., Ballotti, R. et al. (2009). Spleen tyrosine kinase functions as a tumor suppressor in melanoma cells by inducing senescence-like growth arrest. *Cancer Res.* **69**, 2748-2756.

Beronja, S., Livshits, G., Williams, S. and Fuchs, E. (2010). Rapid functional dissection of genetic networks via tissue-specific transduction and RNAi in mouse embryos. *Nat. Med.* **16**, 821-827.

Besse, A., Campos, A. D., Webster, W. K. and Darnay, B. G. (2007). TRAF-interacting protein (TRIP) is a RING-dependent ubiquitin ligase. *Biochem. Biophys. Res. Commun.* **359**, 660-664.

Bignell, G. R., Warren, W., Seal, S., Takahashi, M., Rapley, E., Barfoot, R., Green, H., Brown, C., Biggs, P. J., Lakhani, S. R. et al. (2000). Identification of the familial cylindromatosis tumour-suppressor gene. *Nat. Genet.* **25**, 160-165.

Chapard, C., Hohl, D. and Huber, M. (2012). The role of the TRAF-interacting protein in proliferation and differentiation. *Exp. Dermatol.* **21**, 321-326.

Collin, P., Nashchekina, O., Walker, R. and Pines, J. (2013). The spindle assembly checkpoint works like a rheostat rather than a toggle switch. *Nat. Cell Biol.* **15**, 1378-1385.

Coopman, P. J., Do, M. T., Barth, M., Bowden, E. T., Hayes, A. J., Basyuk, E., Blancato, J. K., Vezza, P. R., McLeskey, S. W., Mangeat, P. H. et al. (2000). The Syk tyrosine kinase suppresses malignant growth of human breast cancer cells. *Nature* **406**, 742-747.

Dikic, I., Wakatsuki, S. and Walters, K. J. (2009). Ubiquitin-binding domains – from structures to functions. *Nat. Rev. Mol. Cell Biol.* **10**, 659-671.

Draviam, V. M., Stegmeier, F., Nalepa, G., Sowa, M. E., Chen, J., Liang, A., Hannon, G. J., Sorger, P. K., Harper, J. W. and Elledge, S. J. (2007). A functional genomic screen identifies a role for TAO1 kinase in spindle-checkpoint signalling. *Nat. Cell Biol.* **9**, 556-564.

Dundr, M., Meier, U. T., Lewis, N., Rekosh, D., Hammarskjöld, M. L. and Olson, M. O. (1997). A class of nonribosomal nucleolar components is located in chromosome periphery and in nucleolus-derived foci during anaphase and telophase. *Chromosoma* **105**, 407-417.

Foley, E. A. and Kapoor, T. M. (2013). Microtubule attachment and spindle assembly checkpoint signalling at the kinetochore. *Nat. Rev. Mol. Cell Biol.* **14**, 25-37.

Heinrich, S., Geissen, E. M., Kamenz, J., Trautmann, S., Widmer, C., Drewe, P., Knop, M., Radde, N., Hasenauer, J. and Hauf, S. (2013). Determinants of robustness in spindle assembly checkpoint signalling. *Nat. Cell Biol.* **15**, 1328-1339.

Hernandez-Verdun, D. (2011). Assembly and disassembly of the nucleolus during the cell cycle. *Nucleus* **2**, 189-194.

Hernandez-Verdun, D. and Gautier, T. (1994). The chromosome periphery during mitosis. *BioEssays* **16**, 179-185.

Holland, A. J. and Cleveland, D. W. (2012). Losing balance: the origin and impact of aneuploidy in cancer. *EMBO Rep.* **13**, 501-514.

Hübner, N. C., Wang, L. H., Kaulich, M., Descombes, P., Poser, I. and Nigg, E. A. (2010). Re-examination of siRNA specificity questions role of PICH and Tao1 in the spindle checkpoint and identifies Mad2 as a sensitive target for small RNAs. *Chromosoma* **119**, 149-165.

Khodjakov, A. and Pines, J. (2010). Centromere tension: a divisive issue. *Nat. Cell Biol.* **12**, 919-923.

Klebig, C., Korinth, D. and Meraldi, P. (2009). Bub1 regulates chromosome segregation in a kinetochore-independent manner. *J. Cell Biol.* **185**, 841-858.

Kops, G. J., Weaver, B. A. and Cleveland, D. W. (2005). On the road to cancer: aneuploidy and the mitotic checkpoint. *Nat. Rev. Cancer* **5**, 773-785.

Lee, S. Y., Lee, S. Y. and Choi, Y. (1997). TRAF-interacting protein (TRIP): a novel component of the tumor necrosis factor receptor (TNFR)- and CD30-TRAF signaling complexes that inhibits TRAF2-mediated NF-kappaB activation. *J. Exp. Med.* **185**, 1275-1286.

Lee, D. A., Grossman, M. E., Schneiderman, P. and Celebi, J. T. (2005). Genetics of skin appendage neoplasms and related syndromes. *J. Med. Genet.* **42**, 811-819.

Lim, S., Kawamura, E., Fielding, A. B., Maydan, M. and Dedhar, S. (2013). Integrin-linked kinase regulates interphase and mitotic microtubule dynamics. *PLoS ONE* **8**, e53702.

Ma, N., Matsunaga, S., Takata, H., Ono-Maniwa, R., Uchiyama, S. and Fukui, K. (2007). Nucleolin functions in nucleolus formation and chromosome congression. *J. Cell Sci.* **120**, 2091-2105.

Matsunaga, S. and Fukui, K. (2010). The chromosome peripheral proteins play an active role in chromosome dynamics. *Biomol. Concepts* **1**, 157-164.

McClelland, S. E., Borusu, S., Amaro, A. C., Winter, J. R., Belwal, M., McAinsh, A. D. and Meraldi, P. (2007). The CENP-A NAC/CAD kinetochore complex controls chromosome congression and spindle bipolarity. *EMBO J.* **26**, 5033-5047.

Mchedlishvili, N., Wieser, S., Holtackers, R., Mouysset, J., Belwal, M., Amaro, A. C. and Meraldi, P. (2012). Kinetochores accelerate centrosome separation to ensure faithful chromosome segregation. *J. Cell Sci.* **125**, 906-918.

Meraldi, P. and Sorger, P. K. (2005). A dual role for Bub1 in the spindle checkpoint and chromosome congression. *EMBO J.* **24**, 1621-1633.

Meraldi, P., Draviam, V. M. and Sorger, P. K. (2004). Timing and checkpoints in the regulation of mitotic progression. *Dev. Cell* **7**, 45-60.

Merkle, J. A., Rickmyre, J. L., Garg, A., Loggins, E. B., Jodoin, J. N., Lee, E., Wu, L. P. and Lee, L. A. (2009). no poles encodes a predicted E3 ubiquitin ligase required for early embryonic development of Drosophila. *Development* **136**, 449-459.

Michel, L. S., Liberal, V., Chatterjee, A., Kirchwegger, R., Pasche, B., Gerald, W., Dobles, M., Sorger, P. K., Murty, V. V. and Benezra, R. (2001). MAD2 haplo-insufficiency causes premature anaphase and chromosome instability in mammalian cells. *Nature* **409**, 355-359.

Moroni, M., Soldatenkov, V., Zhang, L., Zhang, Y., Stoica, G., Gehan, E., Rashidi, B., Singh, B., Ozdemirli, M. and Mueller, S. C. (2004). Progressive loss of Syk and abnormal proliferation in breast cancer cells. *Cancer Res.* **64**, 7346-7354.

Musacchio, A. and Salmon, E. D. (2007). The spindle-assembly checkpoint in space and time. *Nat. Rev. Mol. Cell Biol.* **8**, 379-393.

Nalepa, G., Barnholtz-Sloan, J., Enzor, R., Dey, D., He, Y., Gehlhausen, J. R., Lehmann, A. S., Park, S. J., Yang, Y., Yang, X. et al. (2013). The tumor suppressor CDKN3 controls mitosis. *J. Cell Biol.* **201**, 997-1012.

Park, E. S., Choi, S., Kim, J. M., Jeong, Y., Choe, J., Park, C. S., Choi, Y. and Rho, J. (2007). Early embryonic lethality caused by targeted disruption of the TRAF-interacting protein (TRIP) gene. *Biochem. Biophys. Res. Commun.* **363**, 971-977.

Perera, D., Tilston, V., Hopwood, J. A., Barchi, M., Boot-Handford, R. P. and Taylor, S. S. (2007). Bub1 maintains centromeric cohesion by activation of the spindle checkpoint. *Dev. Cell* **13**, 566-579.

Pines, J. (2011). Cubism and the cell cycle: the many faces of the APC/C. *Nat. Rev. Mol. Cell Biol.* **12**, 427-438.

Regamey, A., Hohl, D., Liu, J. W., Roger, T., Kogerman, P., Toftgard, R. and Huber, M. (2003). The tumor suppressor CYLD interacts with TRIP and regulates negatively nuclear factor kappaB activation by tumor necrosis factor. *J. Exp. Med.* **198**, 1959-1964.

Rieder, C. L., Schultz, A., Cole, R. and Sluder, G. (1994). Anaphase onset in vertebrate somatic cells is controlled by a checkpoint that monitors sister kinetochore attachment to the spindle. *J. Cell Biol.* **127**, 1301-1310.

Santaguida, S. and Musacchio, A. (2009). The life and miracles of kinetochores. *EMBO J.* **28**, 2511-2531.

Sigoillot, F. D., Lyman, S., Huckins, J. F., Adamson, B., Chung, E., Quattrochi, B. and King, R. W. (2012). A bioinformatics method identifies prominent off-targeted transcripts in RNAi screens. *Nat. Methods* **9**, 363-366.

Stegmeier, F., Rape, M., Draviam, V. M., Nalepa, G., Sowa, M. E., Ang, X. L., McDonald, E. R., III, Li, M. Z., Hannon, G. J., Sorger, P. K. et al. (2007a). Anaphase initiation is regulated by antagonistic ubiquitination and deubiquitination activities. *Nature* **446**, 876-881.

Stegmeier, F., Sowa, M. E., Nalepa, G., Gygi, S. P., Harper, J. W. and Elledge, S. J. (2007b). The tumor suppressor CYLD regulates entry into mitosis. *Proc. Natl. Acad. Sci. USA* **104**, 8869-8874.

Su, A. I., Wiltshire, T., Batalov, S., Lapp, H., Ching, K. A., Block, D., Zhang, J., Soden, R., Hayakawa, M., Kreiman, G. et al. (2004). A gene atlas of the mouse and human protein-encoding transcriptomes. *Proc. Natl. Acad. Sci. USA* **101**, 6062-6067.

Sun, L., Gao, J., Huo, L., Sun, X., Shi, X., Liu, M., Li, D., Zhang, C. and Zhou, J. (2010). Tumour suppressor CYLD is a negative regulator of the mitotic kinase Aurora-B. *J. Pathol.* **221**, 425-432.

Toso, A., Winter, J. R., Garrod, A. J., Amaro, A. C., Meraldi, P. and McAinsh, A. D. (2009). Kinetochore-generated pushing forces separate centrosomes during bipolar spindle assembly. *J. Cell Biol.* **184**, 365-372.

Uzunova, K., Dye, B. T., Schutz, H., Ladurner, R., Petzold, G., Toyoda, Y., Jarvis, M. A., Brown, N. G., Poser, I., Novatchkova, M. et al. (2012). APC15 mediates CDC20 autoubiquitylation by APC/C(MCC) and disassembly of the mitotic checkpoint complex. *Nat. Struct. Mol. Biol.* **19**, 1116-1123.

Van Hooser, A. A., Yuh, P. and Heald, R. (2005). The perichromosomal layer. *Chromosoma* **114**, 377-388.

Wallace, H. A., Merkle, J. A., Yu, M. C., Berg, T. G., Lee, E., Bosco, G. and Lee, L. A. (2014). TRIP/NOPO E3 ubiquitin ligase promotes ubiquitylation of DNA polymerase η. *Development* **141**, 1332-1341.

Welchman, R. L., Gordon, C. and Mayer, R. J. (2005). Ubiquitin and ubiquitin-like proteins as multifunctional signals. *Nat. Rev. Mol. Cell Biol.* **6**, 599-609.

Westhorpe, F. G., Diez, M. A., Gurden, M. D., Tighe, A. and Taylor, S. S. (2010). Re-evaluating the role of Tao1 in the spindle checkpoint. *Chromosoma* **119**, 371-379.

Wiznerowicz, M. and Trono, D. (2003). Conditional suppression of cellular genes: Lentivirus vector-mediated drug-inducible RNA interference. *J. Virol.* **77**, 8957-8961.

Zhou, Q. and Geahlen, R. L. (2009). The protein-tyrosine kinase Syk interacts with TRAF-interacting protein TRIP in breast epithelial cells. *Oncogene* **28**, 1348-1356.

Journal of Cell Science

Supplementary Figures

Supplementary Figure S1: RNA interference in HeLa cells. Analysis of mRNA (A-C) and protein (A-B) levels were analyzed by quantitative PCR and immunoblot 24h after siRNA-transfection of HeLa cells. Results are reported as representative mean±s.d. of 2 or more independent experiments.

Supplementary Figure S2: TRAIP-GFP is a functional fusion protein. (A) Western blot of TRAIP-GFP (IB: TRAIP) and HA-ubiquitin (IB: HA) after immunoprecipitation of TRAIP-GFP from 293T cells transfected with pCMV-TRAIPGFP and/or pHA-Ub. B) Confocal images of cells after immuno-staining for GFP (green) and nucleolin (red). Scale bar = 10μm.

Suppl. Figure S1

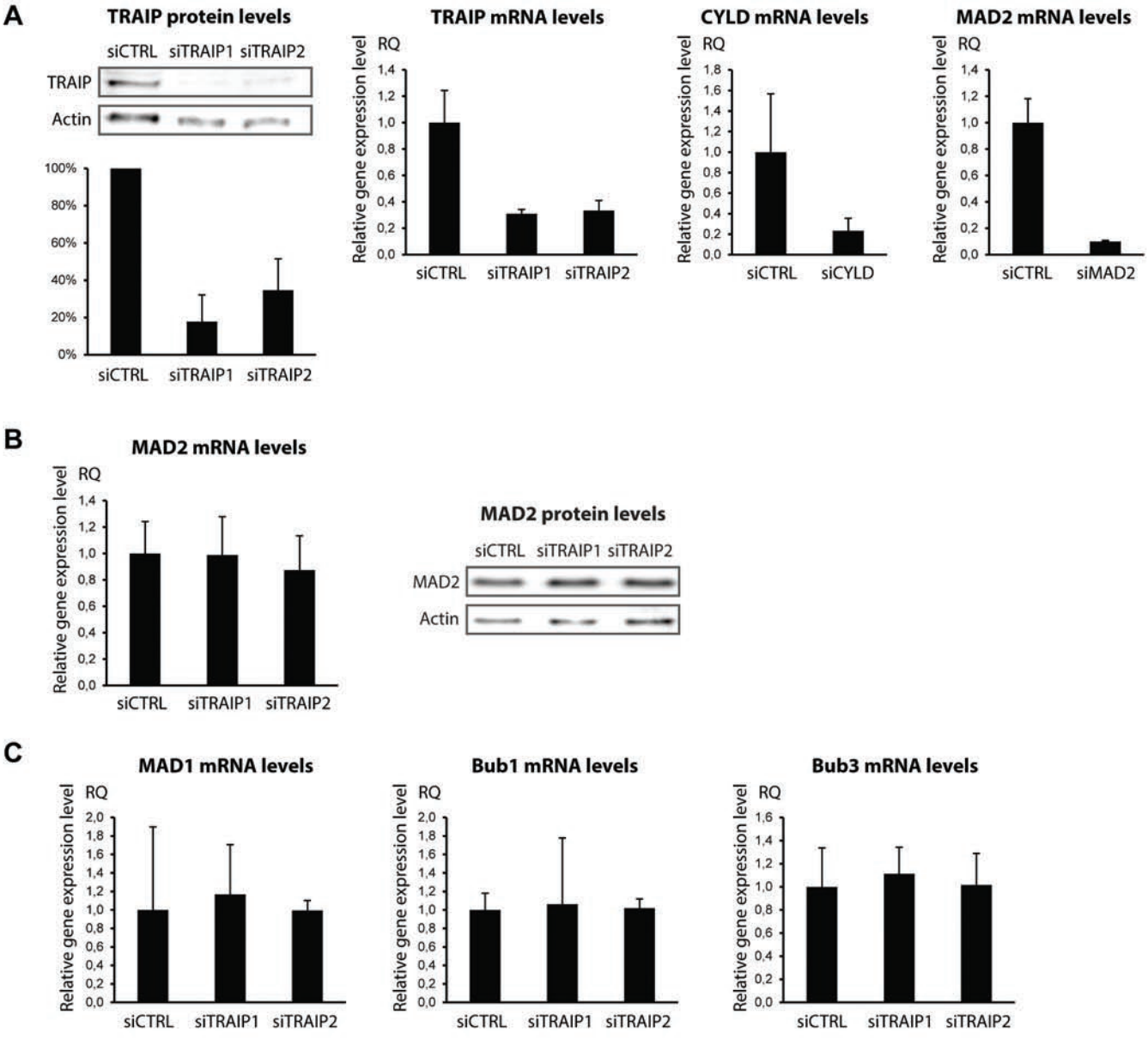

Suppl. Figure S2